Multi-fault diagnosis of gearbox based on resonance-based signal sparse decomposition and comb filter

Zhang, Dingcheng; Yu, Dejie

DOI:
10.1016/j.measurement.2017.03.006

Document Version
Peer reviewed version

Citation for published version (Harvard):
Zhang, D & Yu, D 2017, 'Multi-fault diagnosis of gearbox based on resonance-based signal sparse decomposition and comb filter', *Measurement*, vol. 103, pp. 361-369.
https://doi.org/10.1016/j.measurement.2017.03.006

Multi-Fault Diagnosis of Gearbox Based on Resonance-Based Signal Sparse Decomposition and Comb Filter

Dingcheng Zhang, Dejie Yu

PII: S0263-2241(17)30155-0
DOI: http://dx.doi.org/10.1016/j.measurement.2017.03.006
Reference: MEASUR 4643

To appear in: *Measurement*

Received Date: 29 September 2016
Revised Date: 27 February 2017
Accepted Date: 2 March 2017

Please cite this article as: D. Zhang, D. Yu, Multi-Fault Diagnosis of Gearbox Based on Resonance-Based Signal Sparse Decomposition and Comb Filter, *Measurement* (2017), doi: http://dx.doi.org/10.1016/j.measurement.2017.03.006

Multi-Fault Diagnosis of Gearbox Based on Resonance-Based Signal Sparse Decomposition and Comb Filter

Dingcheng ZHANG[a,b], Dejie YU[a*]

[a] State Key Laboratory of Advanced Design and Manufacturing for Vehicle Body, Hunan University, Changsha, 410082, China
[b] Birmingham Centre for Railway Research and Education, University of Birmingham, Birmingham, B152TT, United Kingdom

Abstract: Fault diagnosis of gearbox is very important for the security and reliability of the equipment. In actual working conditions, multiple faults usually occur in a gearbox. However, the multi-fault diagnosis in gearboxes is a challengeable problem because the signal measured from the gearbox with multiple faults is complex and non-stationary. Particularly, the weaker fault feature signal is generally submerged by the stronger one and background noise. In order to avoid missed diagnosis and misdiagnosis of multi-faults in a gearbox, a novel method called resonance-based signal sparse decomposition (RSSD) with comb filter (CF), namely the RSSD-CF method, is proposed in this paper. The RSSD-CF method is based on the RSSD method which can nonlinearly decompose the vibrational signal of the gearbox with multiple faults into the high resonance component and the low resonance component. To obtain good separation results, the stepwise optimization strategy is applied to the adaptive selection of the optimal decomposition parameters in the RSSD method. In RSSD-CF method, the collected signal is firstly separated into the high and the low resonance components through using the RSSD method with the optimal decomposition parameters. And then, both of the high and the low resonance components are demodulated with the Hilbert transform and the fault information can be found in Hilbert envelop spectra. Finally, CF is constructed to extract the weaker fault feature signal from resonance components and exclude the interference components. The effectiveness of the RSSD-CF method is evaluated by using two experimental cases in this paper. The results confirm the advantage of the proposed method over the traditional RSSD method and the wavelet decomposition for multi-fault diagnosis in gearboxes.

Keywords: Resonance-based signal sparse decomposition (RSSD); stepwise optimization strategy; comb filter (CF); gearbox; fault diagnosis

*Corresponding author. Tel.: +86 731 88821915; fax: +86 731 88823946.
E–mail address: djyu@hnu.edu.cn (Dejie Yu)

1. Introduction

Gearboxes are the main component in various industrial applications. The gearbox failure accounts for 80% in the breakdown of the transmission machinery and the malfunctions of the gearbox are mostly caused by the gear and the bearing faults [1]. Thus, it is of great important to detect the early faults of the gear and the bearing. In actual working conditions, several faults may exist in the gearbox simultaneously. The multi-fault diagnosis of gearboxes is an intractable problem because the weaker fault feature signal is usually buried in the stronger one and background noise.

Recently, many methods have been proposed for the gearbox multi-fault diagnosis, such as the wavelet de-noising and the empirical mode decomposition (EMD) [2], the blind source separation [3], the dual-tree complex wavelet transform [4], the ensemble empirical mode decomposition (EEMD) and the multiwavelet packet [5]. Those methods are based on different centre frequencies and centre frequency bands to decompose the analysis signal. However, the fault feature signals which are caused by multiple faults may have similar centre frequency and overlapping centre frequency bands in the frequency-domain. Thus, the above methods may not be applicable to the multi-fault diagnosis of gearboxes. The RSSD method [6] can be used to separate a signal according to different oscillatory behaviors. In literatures [7-10], RSSD was successfully introduced to the fault diagnosis of gearboxes. However, the weaker fault feature signal may still be submerged in resonance components which are obtained by using the RSSD method in the actual working condition.

The comb filter (CF) is usually applied to the extraction of a periodic signal which is submerged by noise, provided the teeth of the comb coincide with the harmonics of the periodic signal [11-13]. When the fault exists in the gear or the bearing, the periodic impact signal, namely the fault feature signal, will be produced [14]. Thus, the comb filter is a good tool to extract the fault feature signal. Usually, the fundamental frequency of the comb filter is selected as the fault feature frequency. However, it is difficult to use the comb filter if the fault feature frequency cannot be known in advance. Also, filtering the measured signal blindly is a time-consuming process. What's more, the filtering results will be interfered by noises easily.

In this paper, the decomposition parameters in the RSSD method are firstly optimized by using the stepwise optimization strategy. Thus, the vibration signal of the gearbox can be separated into the high and the low resonance components. Then,

both the high and the low resonance components are demodulated with the Hilbert transform. Through setting thresholds for peaks in the envelope demodulation spectra, the suspicious frequency can be found. Next, the suspicious frequency is used as the fundamental frequency to construct the comb filter and then the obtained resonance components are filtered. Finally, the weak fault feature signal can be extract and the interferences can also be identified according those filtered signals. The analysis results of experiments indicate that the RSSD-CF method can be used to extract weak fault feature signals effectively and make the weak fault feature more prominent.

This paper is organized as follows: In section 2, the RSSD method is introduced. In section 3, the method of the construction of comb filters is introduced. The gearbox multi-fault diagnosis based on the RSSD-CF method is introduced in section 4. In section 5, the experimental verification of the proposed method is introduced. The conclusion of this study is given in the last section.

2. Resonance-Based signal sparse decomposition

The RSSD method is actually a sparse representation jointly using the high and the low Q-factor Tunable-Q Wavelet Transforms (TQWT) [6]. To decompose the analysis signal, the morphological component analysis (MCA) is applied in the RSSD method [15].

The quality factor Q denotes the resonance property of a signal

$$Q = \frac{f_o}{BW} \tag{1}$$

where f_o is the center frequency and BW is the bandwidth. The Tunable-Q Wavelet Transform (TQWT) [16] depends on the two-channel bandpass filter banks and adopts the discrete Fourier transform. The center frequency and the corresponding bandwidth of bandpass filter banks is determined by the number of decomposition levels L. As L increases, the center frequency of filter banks f_c

$$f_c = \alpha^j \frac{2-\beta}{4\alpha} f_s, \; j = 1, \cdots, L \tag{2}$$

decreases, and the corresponding bandwidth BW

$$BW = \frac{1}{2} \beta \alpha^{j-1} \pi, \; j = 1, \cdots, L \tag{3}$$

becomes narrower. Therefore, TQWT is actually one kind of wavelet transform of constant Q with a certain degree of redundancy. In Equation (2) and (3), α and β are

the low pass scaling parameter and the high pass scaling parameter respectively, which should satisfy Eq.(4)

$$\beta = \frac{2}{Q+1},\ \alpha = 1-\frac{\beta}{r} \qquad s.t.\ \ 0<\alpha<1,\ \ 0<\beta\le 1,\ \ \alpha+\beta>1 \tag{4}$$

Suppose that the observed signal x can be represented as

$$x = x_1 + x_2 + n \tag{5}$$

where x_1 and x_2 are components with different oscillation behavior, and n is the noise. The Tunable-Q Wavelet Transforms with different Q-factor are used to decompose the observed signal x. The sparse representation process is actually the minimization problem as follow

$$\arg\min_{w_1,w_2} \left\| x-\boldsymbol{\Phi}_1 w_1-\boldsymbol{\Phi}_2 w_2 \right\|_2^2 + \sum_{j=1}^{J_1+1}\lambda_{1,j}\left\| w_{1,j}\right\|_1 + \sum_{j=1}^{J_2+1}\lambda_{2,j}\left\| w_{2,j}\right\|_1 \tag{6}$$

where $\boldsymbol{\Phi}_1$ and $\boldsymbol{\Phi}_2$ represent the inverse TQWT with the high and the low *Q*-factors respectively. w_1 and w_2 represent the transform coefficients of signals x_1 and x_2 under the framework of $\boldsymbol{\Phi}_1$ and $\boldsymbol{\Phi}_2$. J_1 and J_2 are the number of filter banks of high *Q*-factor and low *Q*-factor TQWT, respectively. The regularization parameter vectors $\lambda_{1,j}$ and $\lambda_{2,j}$ are selected by Eq.(7) [17]

$$\begin{cases} \lambda_{1,j} = \theta\left\|\psi_{1,j}\right\|_2 \\ \lambda_{2,j} = (1-\theta)\left\|\psi_{2,j}\right\|_2 \end{cases} \tag{7}$$

where $\psi_{1,j}$ and $\psi_{2,j}$ represent wavelets corresponding to wavelet coefficient $w_{1,j}$ and $w_{2,j}$, respectively. θ has an effect on the energy distribution between the high and the low resonance components. To ensure the balance of the energy distribution of the high and the low resonance components, θ is set to 0.5 in the paper. After w_1 and w_2 are obtained, the estimated high and low resonance components are shown as follows

$$\hat{x}_1 = \boldsymbol{\Phi}_1 w_1^*, \quad \hat{x}_2 = \boldsymbol{\Phi}_2 w_2^* \tag{8}$$

For multi-fault diagnosis, when the gear or the bearing has faults in the gearbox, fault feature signals can be found in the low resonance component by using the RSSD method [10]. When both the gear and the bearing have faults, the fault feature signals of the gear and the bearing can be separated into the high and the low resonance components respectively by using the RSSD method. The main reason is that the fault feature signal of the gear has better frequency aggregation than that of the bearing [18]. Thus, the RSSD method is a good tool to detect the multiple faults in gearboxes.

However, it is important to adaptively select the parameters of RSSD according to the feature of the analysis signal because those parameters have a great impact on the decomposition results. For RSSD, six parameters need to be determined, namely the high and the low quality factors Q_1 and Q_2, the high and the low redundancies r_1 and r_2, the high and the low decomposition levels J_1 and J_2. In this study, both r_1 and r_2 are set to be 5 by considering the redundancy and complex calculations. To assure that all the information of analysis signal is included in the subsignals, the maximum number of decomposition levels $J_{\max}$ is employed in this paper. $J_{\max}$ is defined as [16]

$$J_{\max} = \left\lfloor \frac{\log\left(\frac{N}{4(Q+1)}\right)}{\log\left(\frac{Q+1}{Q+1-2/\mathrm{r}}\right)} \right\rfloor \tag{9}$$

where $\lfloor \bullet \rfloor$ represents the rounding operation.

Therefore, how to adaptively select quality factors is the key problem in the RSSD method. In this paper, the stepwise optimization strategy is firstly applied to optimizing Q_1 and Q_2. This strategy which is widely used to solve the multi-variable optimal problem can turn a multi-variable problem into several sub-problems through dividing variables into several groups [19-21]. Actually, two steps are adopted to obtain the optimal quality factors in the optimization process. The first step is that the high quality factor is optimized and the low quality factor is set as 1. Then, the low quality factor is optimized and the high quality factor is fixed as the obtained optimal value in the first step. Finally, the optimal high factor and the optimal low quality factor can be obtained through using the above two steps.

The following objective function F [18] is taken as the evaluation index in this strategy

$$F = \alpha_1 \times SI(x_1) + \alpha_2 \times Kur(x_2) \tag{10}$$

where F is the composite index. $SI(x_1)$ is the smoothness index of the high resonance component, which is calculated by Eq.(11). $Kur(x_2)$ is the kurtosis of the low resonance component, which is calculated based on Eq.(12). α_1 and α_2 are the weight coefficients of smoothness index and the kurtosis, respectively.

$$SI(x)=\frac{\exp\left(\sum_{i=1}^{N}\ln\left(x_i\right)\Big/N\right)}{\sum_{i=1}^{N}x_i\Big/N} \tag{11}$$

$$Kur(x)=\frac{E\{(x-\mu)^4\}}{\sigma^4} \tag{12}$$

The values α_1 and α_2 are selected according to the impact characteristic of analysis signals, i.e. Eq.(13). If the impact characteristic of signals is obvious, the value of α_1 should be increased appropriately. Otherwise, if the oscillatory behavior of signals is obvious, then the values of α_2 should be increased appropriately.

$$\begin{aligned}\alpha_1&=\begin{cases}\dfrac{\lfloor Kur(\mathrm{x})\rfloor}{10} & Kur(\mathrm{x})<10\\ 0.9 & Kur(\mathrm{x})\geq 10\end{cases}\\ \alpha_2&=1-\alpha_1\end{aligned} \tag{13}$$

Therefore, the adaptive selection process of decomposition parameters of RSSD can be turn into the maximization process as follow, according to equations (6) and (10).

$$\begin{aligned}&\max \quad F(Q_1,Q_2)\\ &\text{s.t.}\quad Q_1,Q_2\in R\\ &\qquad Q_1>Q_2\geq 1\end{aligned} \tag{14}$$

To show the effectiveness of the RSSD method with optimized decomposition parameters, a simulation signal as shown in Fig. 1 (a) is considered. The simulation signal is composed of the noises, the fault feature signals of the gear and the bearing. The gear fault feature signal has the high resonance behavior, whereas the bearing fault feature signal has the low resonance behavior [18]. The Hilbert envelope spectrum of Fig.1 (a) is shown in Fig.1 (b), which is obtained by the Fourier transform of the envelop signal $B(t)$

$$B(t)=\sqrt{x^2(\mathrm{t})+\mathrm{H}^2[x(t)]} \tag{15}$$

where $x(t)$ is the analysis signal, $\mathrm{H}[x(t)]$ represents the Hilbert transform of the analysis signal.

The simulated rotating and outer bearing fault frequencies of the simulation signal shown in Fig. 1 (a) are $f_r=40Hz$ and $f_o=95Hz$, respectively. Obvious peaks can be found at f_r and $2f_r$ in Fig.1 (b), which indicates the existence of the gear fault. However, there is no obvious peak at the bearing fault feature frequency

f_o in Fig.1 (b) because the bearing fault is too weak. Thus, the bearing fault information is submerged.

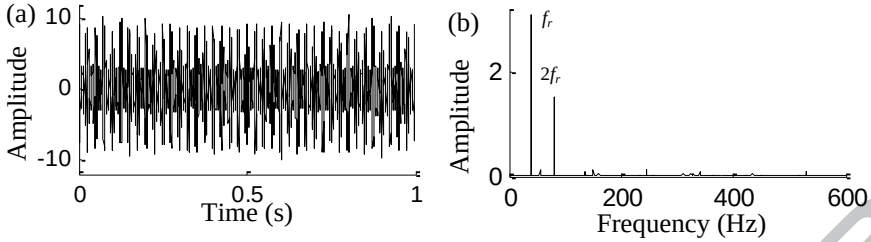

Fig. 1 The time domain waveform and the Hilbert envelope spectrum of the simulated signal

The decomposition parameters of the RSSD method are adaptively selected by using the stepwise optimization strategy, and the obtained optimal decomposition parameters are Q_1=8.24 and Q_2=1. The high and the low resonance component can be obtained through using the RSSD method with the obtained optimal parameter, which are shown in Fig.2 (a) and 2 (c) respectively. Fig. 2 (b) and 2 (d) are the Hilbert envelope spectra of resonance components. It can be seen from Fig. 2 (d) that obvious peaks exist at f_o and its harmonics which suggest the existence of the bearing fault. The analysis results of the simulation example indicate that the stepwise optimization strategy can be successfully applied to the parameter selection of the RSSD method. However, the collected signal is complex in actual working condition. The weaker fault information may still not be found in the resonance components. In this paper, the comb filtering method is introduced to extract the weaker fault feature signal.

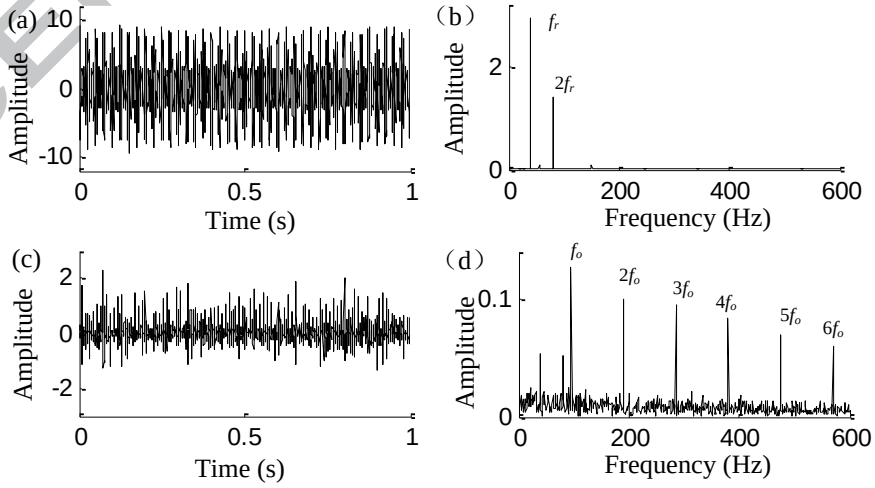

Fig. 2 RSSD of the simulated signal and the Hilbert envelope spectra of resonance components. (a) & (c) The high resonance component and the low resonance component; (b) & (d) The Hilbert envelope spectra of (a) and (c)

3 Comb filter

In the above section, the RSSD method is applied to making the weaker fault more prominent. In the practical operating condition, the interference components may still exist in the resonance components, which easily results in missed diagnosis and misdiagnosis. In order to exclude the interference components and extract the weaker fault feature signal, the comb filter is constructed based on the Fourier kernel function in this paper. The Fourier kernel function is defined as

$$\mathrm{s}(t)=\frac{\sin k_0 t}{\pi t} \tag{16}$$

The Fourier transform of $s(t)$ is

$$\mathrm{S}(k)=\begin{cases}1 & (|k|\le k_0,\ k_0\ge 0)\\ 0 & (k>k_0,\ k<-k_0)\end{cases} \tag{17}$$

Therefore, the Fourier kernel function is a band-pass filter with the amplitude value of 1. According to the property of the Fourier transform, the function $\mathrm{s}(t)\exp(j2\pi f_c t)$ represents an ideal comb filter whose bandwidth and fundamental frequency are $2k_0$ and f_c, respectively. As the filtering results are insensitive to the bandwidth parameter $2k_0$, the bandwidth of comb filter is set to 30Hz. Thus, the comb filter in this paper is defined as

$$h(\mathrm{t})=\frac{\sin k_o t}{\pi t}\times\sum_{i=1}^{n}\exp(\mathrm{j}2\pi \mathrm{i} f_c t) \tag{18}$$

The fault feature signal in the gearbox is actually the periodic impact signal. If the fault feature frequency is selected as the fundamental frequency of the comb filter, the fault feature signal can be extracted by filtering the resonance components. And then, the fault in the gearbox can be detected. However, if the fundamental frequency of the comb filter is not the fault feature frequency in the gearbox, the filtered signal will not be a periodic impact signal. In this paper, the fundamental frequency of CF is selected as the suspicious fault feature frequency. Supposed that the spectrum peak value at j Hz in the Hilbert envelop spectrum is P_j ($0<j<\frac{f_s}{2}$, f_s is the sampling frequency), the threshold T_j for the spectrum peak P_j is established as follow to found the suspicious fault feature frequency

$$T_j=\sigma\left(\frac{P_{j-1}+P_{j+1}}{2}\right) \tag{19}$$

where σ is set to1.8 according to our experimental experiences. If P_j is greater than T_j, the frequency j Hz will be consider as the suspicious frequency. The comb filter is successfully applied to the multi-fault diagnosis in the gearbox and its effectiveness is proved by the below experimental cases.

4 Resonance-Based Signal Sparse Decomposition with Comb Filter for Gearbox Multi-Fault Diagnosis

To avoid missed diagnosis and misdiagnosis in the gearbox, the RSSD-CF method is proposed in this paper. The RSSD method is firstly used to decompose the vibrational signal of the gearbox into the high resonance component and the low resonance component. Then, the Hilbert transform demodulation method is applied to the analysis of the obtained resonance components. Through setting thresholds in the envelope demodulation spectra, the suspicious frequency can be found. Next, the suspicious frequency is selected as the fundamental frequency to construct the comb filter which is applied to filtering the obtained resonance components. Finally, the weaker fault feature component can be extracted and the interference components can also be identified according to those filtered signals. The schematic diagram of the gearbox multi-fault diagnosis based on the RSSD-CF method is shown in figure 3.

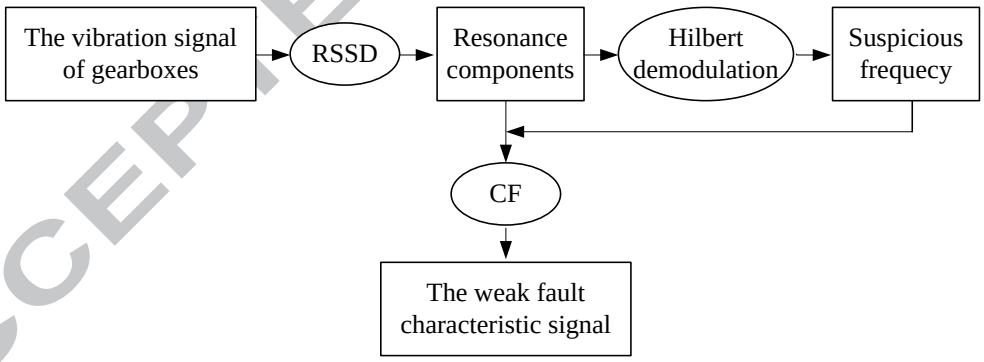

Fig. 3 Schematic diagram of the proposed method

5 Experimental validations

To verify the validity of the proposed method, this section presents two application cases of the multi-fault diagnosis of gearboxes. The case 1 includes the outer race fault and the inner race fault in two different bearings. The case 2 includes the outer race fault in the bearing and the gear tooth crack in the gear. The fault simulator is shown in Fig. 4.

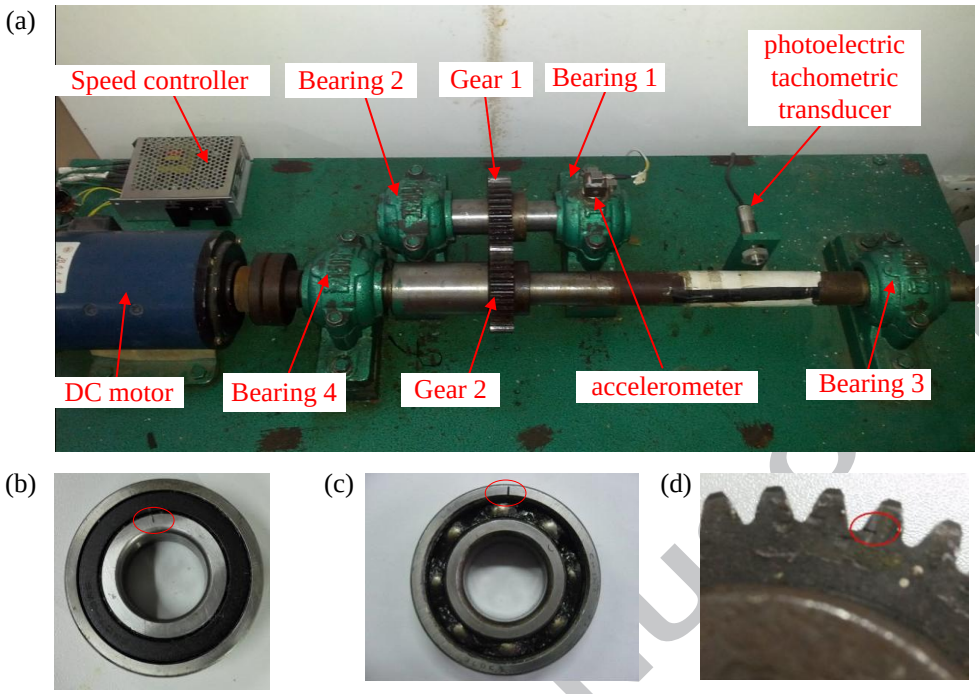

Fig. 4 Test platform. (a) The gearbox fault simulation bench; (b) The bearing with the inner race fault; (c) The bearing with outer race fault; (d) The gear with the teeth crack

The deep groove ball bearing was used in the experiment. The experimental bearing parameters are shown in Table 1. To simulate the inner race fault of the bearing, a slot with the width of 0.15mm and depth of 1.5 mm was made at the inner race as shown in Fig.4 (b). To simulate the outer race fault of the bearing, a slot with the width of 0.15mm and depth of 3mm was made at the outer race as shown in Fig. 4 (c). The spur gear was used in the experiment. In order to simulate the gear with the tooth crack, a slot with the width of 0.15mm and depth of 1 mm was made at the gear tooth root as shown in Fig. 4 (d). The acceleration sensor was installed on the pedestal of bearing 1.

Table 1
Parameters of the experimental bearing

Type	Outer race diameter	Ball diameter	Number of balls	Contact angle
SKF6307-2RS	80mm	13.5mm	8	0^o

5.1 Case1: The outer race fault in bearing 1 and the inner race fault in bearing 2

In this case, there are an outer race fault and an inner race fault in bearing 1 and bearing 2 respectively. The shaft rotating speed is fixed at 1500rpm (i.e. f_r=25Hz). The sampling frequency was 8192Hz and the number of sampling points is 8192.

Hence, the fault feature frequency of bearing's outer race is f_o = 76.5Hz and the fault feature frequency of bearing's inner race is f_i =123.5Hz. The time domain waveform and the envelop spectrum of the vibration signal of case 1 are shown in Fig. 5 (a) and Fig. 5 (b), respectively. The obvious peak values appear only at the rotating frequency f_r, the fault feature frequency of outer race f_o and its harmonics in Fig. 5 (b). Through observing the envelop spectrum, the outer race fault can be detected, but the inner race fault could not be identified because the peaks at f_i and its harmonics are not obvious.

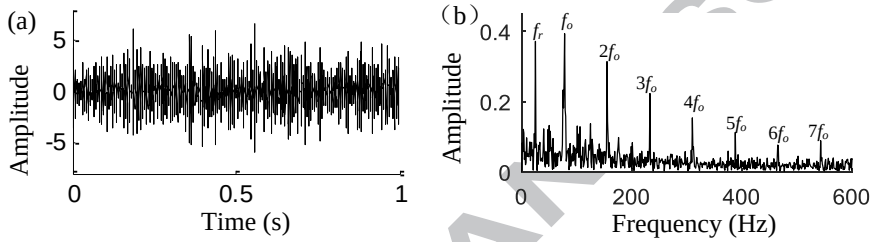

Fig. 5 The time domain waveform and the Hilbert envelope spectrum of the vibration signal of case 1

The collected signal as shown in Fig. 5 (a) is subject to the RSSD method. The value of the optimal decomposition parameters Q_1, Q_2 are 18.71 and 1.0. The analysis results are shown in Fig. 6. Fig. 6 (b) and Fig. 6 (d) are the Hilbert envelope spectra of decomposed components shown in Fig. 6 (a) and Fig. 6 (c), respectively. The outer race fault can be detected because there are obvious peaks at f_0 and it's harmonics in Fig 6(b). In Fig. 6 (d), there are obvious peaks at f_r and it's harmonics, f_0 and it's harmonics. Besides, obvious peaks can be seen at the fault characteristic frequency of inner race f_i and 101Hz as well. As f_r is the rotating frequency and f_0 is the fault feature frequency of the outer race fault, the frequencies of f_r and f_0 in Fig 6(d) are not suspicious frequencies and should not be selected as the fundamental frequency of CF. However, the bearing inner race fault could not be absolutely identified because there are no obvious peaks at the harmonics of f_i in Fig. 6(d). Also, the interpretation of the obvious peak at 101Hz is unclear. Thus, the fault characteristic frequency of inner race f_i and 101Hz in Fig 6(d) are suspicious frequencies and the obtained low resonance component should be further processed by comb filtering.

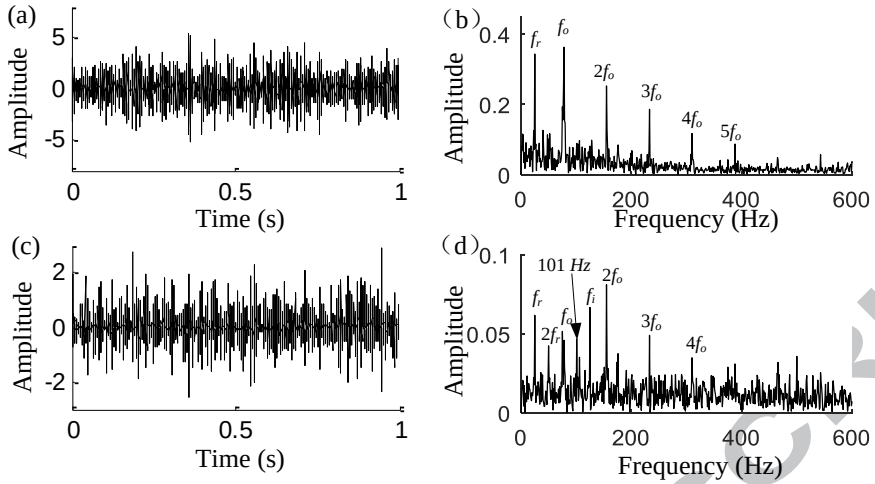

Fig. 6 RSSD of the vibration signal of case 1 and the Hilbert envelope spectra of resonance components. (a) & (c) The high resonance component and the low resonance component; (b) & (d) The Hilbert envelope spectra of (a) and (c)

The low resonance component shown in Fig. 6 (c) is subject to comb filtering. The fundamental frequency of comb filter is the fault feature frequency of inner race f_i. The filtered signal and its Hilbert envelope spectrum are shown in Fig. 7 (a) and Fig. 7 (b) respectively. It can be seen from Fig. 7 (b) that peaks are obvious at the harmonics frequencies of f_i. The time domain waveforms of the collected signal, the low resonance component and the filtered signal in the time interval of 0-0.05s are shown in Fig. 8 (a), (b) and (c), respectively. It can be seen from Fig. 8 that periodicity impulses with the impulse period T_i ($T_i = 1/f_i$) are obvious in the filtered signal. Thus, the RSSD-CF method can be used to detect the inner race fault in the bearing in this case. Also, when the inner race fault occurs in the bearing, peaks are obvious not only at the harmonics frequencies of f_i in the envelop spectrum, but also at the harmonics frequencies of the rotating frequency f_r. Thus, the existent of the obvious peak at f_r in Fig. 6 (b) and (d) is caused by the bearing inner race fault.

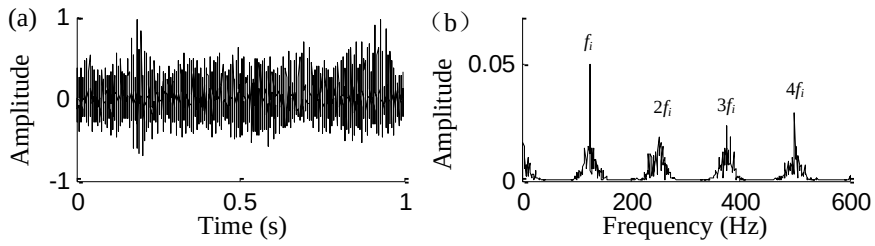

Fig. 7 The filtered result when the fundamental frequency of the comb filter is f_i. (a) The filtered signal; (b) The Hilbert envelope spectrum of the filtered signal

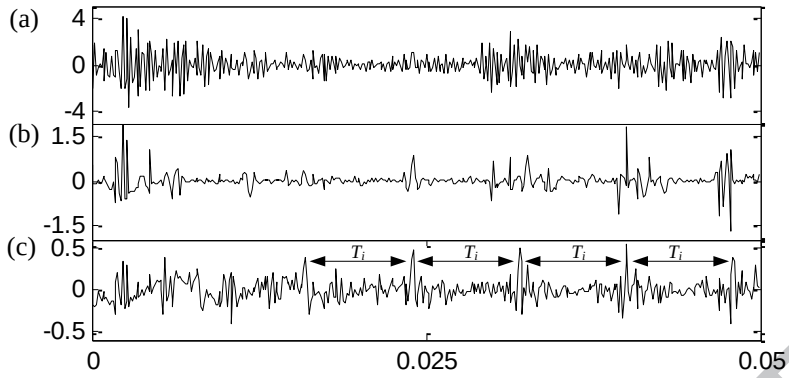

Fig. 8 The time domain waveform of case 1 in 0-0.05s. (a) The vibration signal; (b) The low resonance component; (c) The filtered signal

In addition, there is an obvious peak at 101Hz in the low resonance component shown in Fig. 6 (d). In order to avoid missed diagnosis, the comb filter is constructed with the fundamental frequency f_c=101Hz and then the low resonance component is subject to filtering by using this comb filter. The filtered signal is shown in Fig. 9 (a) and its Hilbert envelope spectrum is shown in Fig. 9 (b). It can be seen from Fig. 9 (b) that the peak values are not obvious at the harmonic frequencies of 101Hz. This indicates that there are no periodicity impulses with the impulse frequency 101Hz and thus the frequency 101Hz is just the interference frequency.

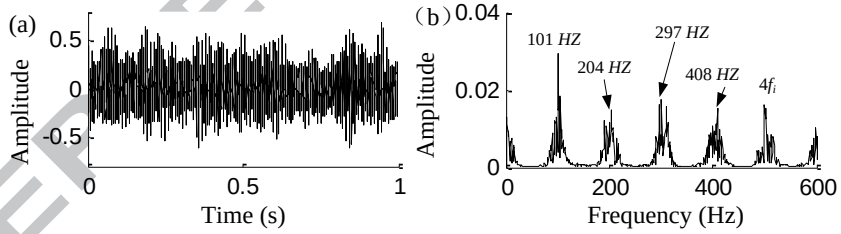

Fig. 9 The filtered result when the fundamental frequency of the comb filter is 101Hz. (a) The filtered signal; (b) The Hilbert envelope spectrum of the filtered signal

Fig. 10 shows the decomposition results at level 5 of the vibrational signal shown in Fig. 5 (a) using db10 wavelet [22]. The obtained sub-signals and their corresponding envelop spectra are shown in Fig. 10 (a) and Fig. 10 (b), respectively. However, there is no obvious peak at f_i in Fig. 10 (b), which indicates that the wavelet decomposition method cannot extract the weaker fault feature signal in this case.

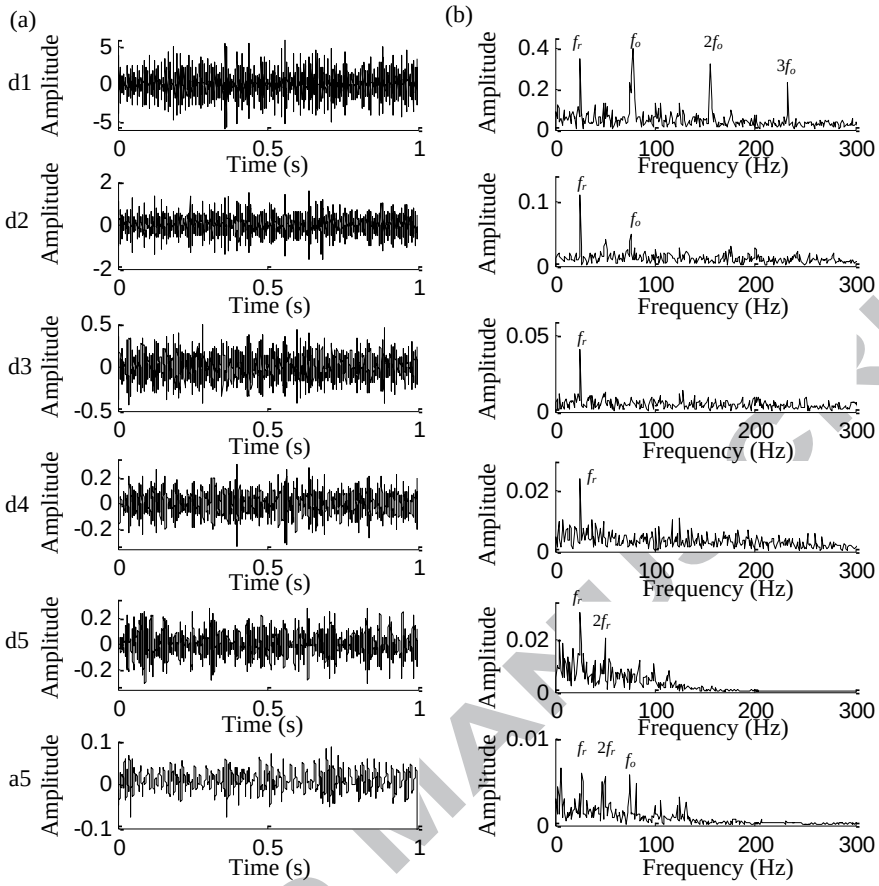

Fig. 10 The wavelet decomposition of the vibration signal of case 1 using db10. (a) The sub-signals and (b) The Hilbert envelope spectra of the sub-signals

5.2 Case2: The outer race fault in bearing 1 and the gear tooth crack in gear 1

In this case, a bearing with outer race fault and a gear with tooth crack are used. The sampling frequency f_s was 8192 Hz and the number of sampling points is 8192. The shaft rotating speed is fixed at 600rpm (i.e. f_r =10Hz). The fault feature frequency of outer race f_o was 30.6 Hz. The time domain waveform of the collected vibration signal is shown in Fig. 11 (a) and the envelope spectrum of the signal is given in Fig. 11 (b). The obvious peak values appear only at f_o and its harmonics in Fig. 11 (b). Thus, the traditional demodulation analysis can not detect the gear fault though the bearing fault is easily identified.

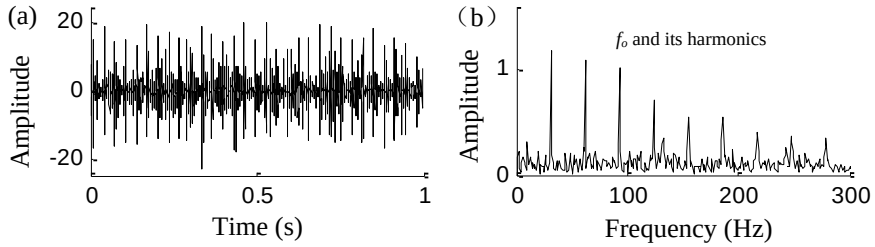

Fig. 11 The time domain waveform and the Hilbert envelope spectrum of the vibration signal of case 2

The collected signal as shown in Fig. 11 (a) is subject to the RSSD method. The value of the optimal decomposition parameters Q_1, Q_2 are 41.03 and 9.04, respectively. The analysis results are shown in Fig. 12. Fig. 12 (b) and Fig. 12 (d) are the Hilbert envelope spectra of resonance components shown in Fig. 12 (a) and Fig. 12 (c), respectively. In Fig. 12 (b), there are obvious peaks at f_o and its harmonics. Thus, the bearing outer race fault can be detected. It also can be seen from Fig. 12 (b) that obvious peaks exist at f_r and 132 Hz. However, the gear fault could not be identified because the obvious peaks at the harmonics of f_r do not exist in Fig. 12 (b). Also, other kinds of faults, like inner race faults in bearings, will generate obvious peak values exist at f_r and its harmonics as well. What's more, the interpretation of the obvious peak at 132Hz is unclear. Thus, the comb filtering is used to further process the high resonance component in the case.

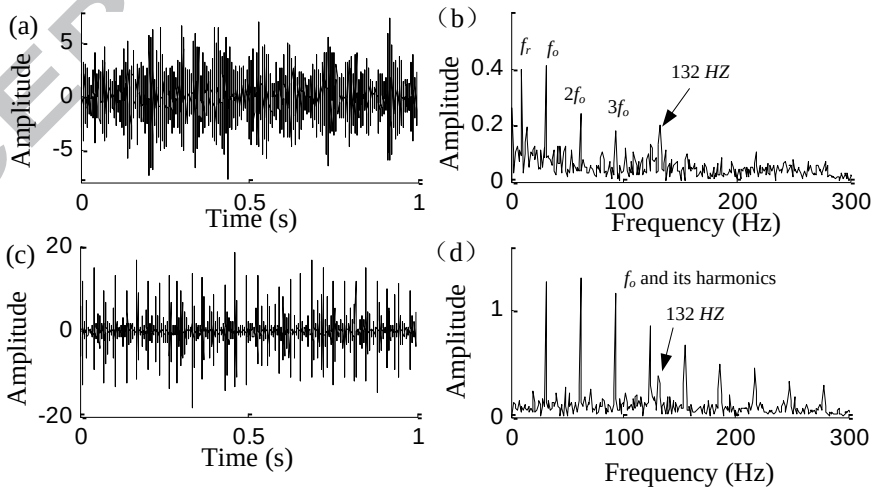

Fig. 12 RSSD of the vibration signal of case 2 and the Hilbert envelope spectra of resonance components. (a) & (c) The high resonance component and the low resonance component; (b) & (d) The Hilbert envelope spectra of (a) and (c)

The high resonance component shown in Fig. 12 (a) is subject to comb filtering. The fundamental frequency of comb filter f_c is the rotating frequency f_r. The

filtered signal is shown in Fig. 13 (a) and its Hilbert envelope spectrum is shown in Fig. 13 (b). The periodicity impulses with the impulse period T_r ($T_r = 1/f_r$) are obvious in the filtered signal as shown in Fig. 13 (a). In Fig. 13 (b), obvious peaks can be found at f_r and its harmonics. The low resonance component shown in Fig. 12 (c) is filtered by the comb filter with the fundamental frequency f_c=132Hz. The filtered signal and its Hilbert envelope spectrum are shown in Fig. 14. There is no obvious peak at the harmonics of 132Hz in Fig. 14 (b). Thus, 132Hz is not caused by the periodic impact signal, that is, faults in the gearbox. According to the results of these two filtering processes, it can be known that the gear fault exists in the gearbox and the frequency 132Hz is the interference frequency.

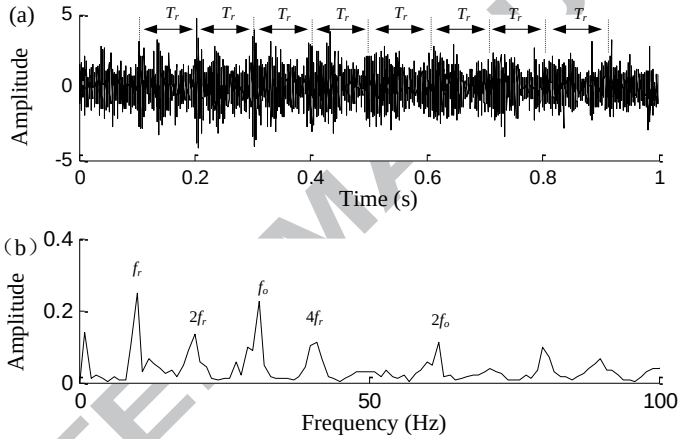

Fig. 13 The filtered result when the fundamental frequency of the comb filter is f_r. (a) The filtered signal; (b) The Hilbert envelope spectrum of the filtered signal

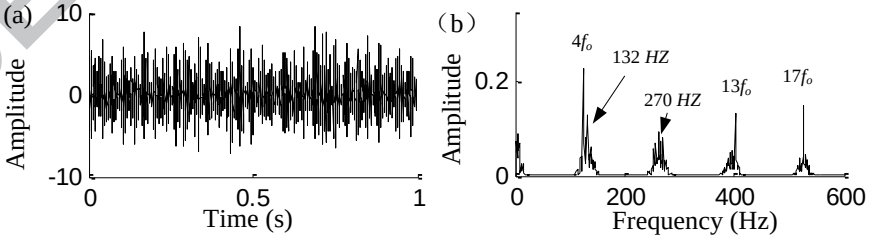

Fig. 14 The filtered result when the fundamental frequency of the comb filter is 132Hz.(a) The filtered signal; (b) The Hilbert envelope spectrum of the filtered signal

The vibrational signal shown in Fig. 11 (a) is decomposed by using db10 wavelet [22] and the decomposition results are shown in Fig 15. The sub-signals and their Hilbert envelop spectra are shown in Fig 15 (a) and Fig 15 (b), respectively. There is no obvious peak at the rotating frequency f_r in Fig 15 (b). Thus, the wavelet

decomposition method cannot make the weaker fault feature more prominent in this case.

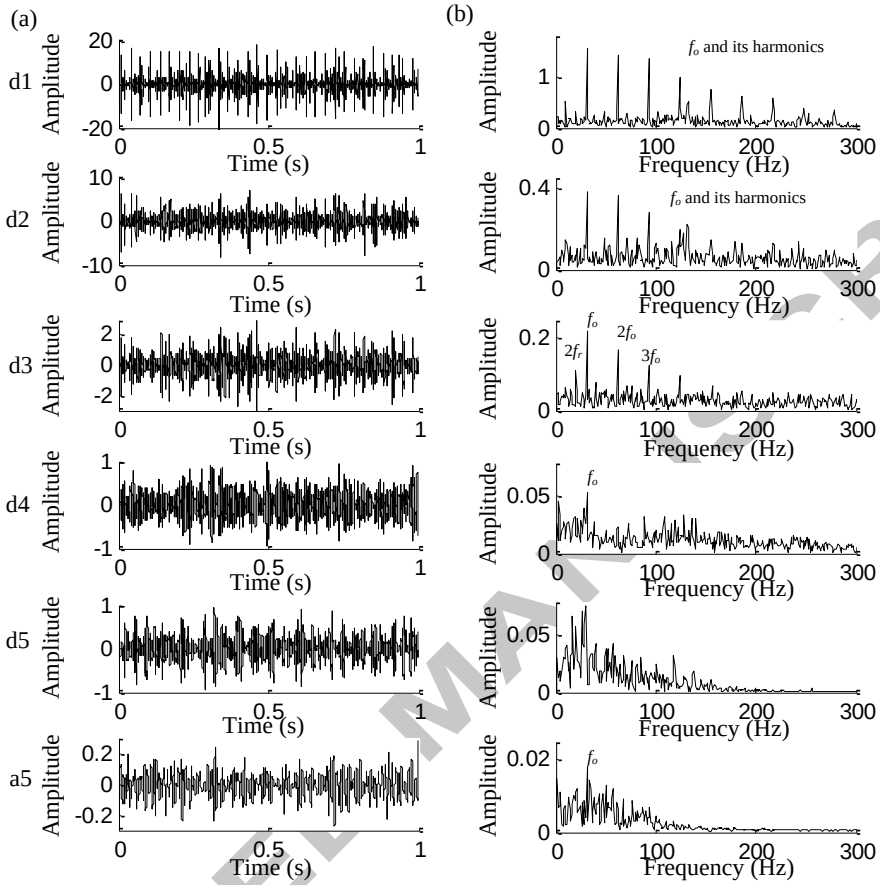

Fig. 15 The wavelet decomposition of the vibration signal of case 2 using db10. (a) The sub-signals; (b) The Hilbert envelope spectra of the sub-signals

6. Conclusion

To detect multiple faults in gearboxes, a novel method called resonance-based signal sparse decomposition with comb filter (RSSD-CF) is proposed in this paper. The comb filter is a good tool to extract the fault feature signal from the collected vibrational signal. However, the priori knowledge should be known before constructing the comb filter. In this work, the RSSD method is introduced to decompose the vibrational signal and thus the fundamental frequency of the comb filter can be obtained. Further, the stepwise optimization strategy is firstly applied to the parameter optimization of the RSSD method. The decomposition effect of RSSD can be obviously improved by the stepwise optimization strategy. The following conclusions are obtained by combining the analysis results of simulation and experimental signals.

（1）The RSSD-CF method is compared with the traditional Hilbert envelope spectrum method and the wavelet decomposition in this work. The results show that

the RSSD-CF method outperforms the traditional Hilbert envelope spectrum method and the wavelet decomposition for the multi-fault diagnosis in gearboxes.

(2) Comb filter is a good tool to extract the fault feature signal, especially the periodic impact signal. Meanwhile, comb filter can efficiently exclude the interference component and make the weaker fault feature more prominent.

(3) The decomposition parameters of RSSD can be adaptively selected by using the stepwise optimization strategy and then the separating results of RSSD can be greatly improved. Also, comparing with the genetic algorithm [18], the strategy has higher efficiency. For example, in case 1 and case 2, the RSSD-CF method costs 1092s and 1123s respectively, but the method in [18] costs 4251s and 4637s.

Acknowledgements

This study was supported by the National Natural Science Foundation (51275161), China Scholarship Council and the project of Advanced Design and Manufacturing of Automotive Body of Hunan University, which is the independent subject foundation (71375004) of State Key Laboratory. The author especially appreciates the guidance provided by Ivan Selesnick on TQWT tool kit.

References

1. Li, Z., et al., *Virtual prototype and experimental research on gear multi-fault diagnosis using wavelet-autoregressive model and principal component analysis method.* Mechanical Systems and Signal Processing, 2011. **25**(7): p. 2589-2607.
2. Shao, R., W. Hu, and J. Li, *Multi-Fault Feature Extraction and Diagnosis of Gear Transmission System Using Time-Frequency Analysis and Wavelet Threshold De-Noising Based on EMD.* Shock & Vibration, 2013. **20**(4): p. 763-780.
3. Jing, J.P. and G. Meng, *A novel method for multi-fault diagnosis of rotor system.* Mechanism & Machine Theory, 2009. **44**(4): p. 697-709.
4. Wang, Y., Z. He, and Y. Zi, *Enhancement of signal denoising and multiple fault signatures detecting in rotating machinery using dual-tree complex wavelet transform.* Mechanical Systems & Signal Processing, 2010. **24**(1): p. 119-137.
5. Jiang, H., C. Li, and H. Li, *An improved EEMD with multiwavelet packet for rotating machinery multi-fault diagnosis.* Mechanical Systems & Signal Processing, 2013. **36**(2): p. 225-239.
6. Selesnick, I.W., *Resonance-based signal decomposition: A new sparsity-enabled signal analysis method ☆.* Signal Processing, 2011. **91**(12): p. 2793-2809.
7. Chen, X.M., Y.U. De-Jie, and J.S. Luo, *Envelope demodulation method based on resonance-based sparse signal decomposition and its application in roller bearing fault diagnosis.* Zhendong Gongcheng Xuebao/journal of Vibration

Engineering, 2012. **25**(6): p. 628-636.
8. Wang, H., J. Chen, and G. Dong, *Feature extraction of rolling bearing's early weak fault based on EEMD and tunable Q-factor wavelet transform.* Mechanical Systems & Signal Processing, 2014. **48**(1-2): p. 103-119.
9. Cui, L., et al., *Resonance-Based Nonlinear Demodulation Analysis Method of Rolling Bearing Fault.* Advances in Mechanical Engineering, 2015. **5**(5): p. 420694-420694.
10. Cai, G., X. Chen, and Z. He, *Sparsity-enabled signal decomposition using tunable Q-factor wavelet transform for fault feature extraction of gearbox.* Mechanical Systems & Signal Processing, 2013. **41**(s 1–2): p. 34-53.
11. Lim, J.S., A.V. Oppenheim, and L. Braida, *Evaluation of an adaptive comb filtering method for enhancing speech degraded by white noise addition.* IEEE Transactions on Acoustics Speech & Signal Processing, 1978. **26**(4): p. 354-358.
12. Wei, Z., et al., *Single-lead fetal electrocardiogram estimation by means of combining R-peak detection, resampling and comb filter.* Medical Engineering & Physics, 2010. **32**(7): p. 708-19.
13. Wei, Z., et al., *Noninvasive fetal ECG estimation using adaptive comb filter ☆.* Computer Methods & Programs in Biomedicine, 2013. **112**(1): p. 125-134.
14. Li, Z., et al., *Virtual prototype and experimental research on gear multi-fault diagnosis using wavelet-autoregressive model and principal component analysis method.* Mechanical Systems & Signal Processing, 2011. **25**(7): p. 2589-2607.
15. Bobin, J., et al., *Morphological component analysis: an adaptive thresholding strategy.* IEEE Transactions on Image Processing A Publication of the IEEE Signal Processing Society, 2007. **16**(11): p. 2675-2681.
16. Selesnick, I.W., *Wavelet Transform With Tunable Q-Factor.* IEEE Transactions on Signal Processing, 2011. **59**(8): p. 3560-3575.
17. Selesnick, I., *TQWT toolbox guide.* Electrical and Computer Engineering, Polytechnic Institute of New York University. Available online at: http://eeweb. poly. edu/iselesni/TQWT/index. html, 2011.
18. Zhang, D., D. Yu, and W. Zhang, *Energy operator demodulating of optimal resonance components for the compound faults diagnosis of gearboxes.* Measurement Science & Technology, 2015. **26**(11).
19. Putra, Z.A. and K.A. Amminudin, *Two-Step Optimization Approach for Design of A Total Water System.* Industrial & Engineering Chemistry Research, 2008. **47**(16): p. 6045-6057.
20. Santini, F., et al., *A two-step optimization procedure for assessing water constituent concentrations by hyperspectral remote sensing techniques: An application to the highly turbid Venice lagoon waters.* Remote Sensing of Environment, 2010. **114**(4): p. 887-898.
21. Jusko, K.L. and W.P. Shively, *Applying a Two-Step Strategy to the Analysis of Cross-National Public Opinion Data.* Political Analysis, 2005. **13**(4): p. 327-344.
22. Lou, X. and K.A. Loparo. *Bearing fault diagnosis based on wavelet transform and fuzzy inference*. in *Iranian Conference on Fuzzy Systems*. 2006.

Highlights

(1) Using the stepwise optimization strategy to adaptively select parameters of the RSSD method.
(2) Extracting the weak fault feature and excluding the suspicious frequency by using the comb filter firstly.
(3) ARSSD-CF method is firstly proposed for multi-faults diagnosis of gearbox